scientific reports

Check for updates

OPEN

Simultaneous targeted delivery of doxorubicin and KRAS suppression by a hybrid molecule containing miR-143 and AS1411 aptamer

Khanittha Laowichuwakonnukul[1], Boonchoy Soontornworajit[2,3], Jiraporn Arunpanichlert[2,3] & Pichayanoot Rotkrua[1,3]✉

Hybrid molecules can be engineered to target tumors by merging drugs with the same or distinct mechanisms of action. The coexistence of multiple pharmacologically active entities within the cancer cell enhances the therapeutic efficacy of the hybrid molecule compared to single-target inhibitors. *KRAS* is considered the most common oncogenic gene in human cancers and is targeted by tumor suppressor miR-143. Therefore, an increase in miR-143 expression is a promising way to inhibit CRC cell growth. This research aims to develop a hybrid anticancer drug carrier by combining miR-143 and AS1411 aptamers through a hybridization strand (MAH) and loading doxorubicin (Dox), a chemotherapy drug. The uptake capability of MAH into the SW480 CRC cells was confirmed by detecting fluorescence intensity with a fluorescence microscope. After treatment of MAH in SW480 cells, the level of miR-143 was increased, but KRAS expression was decreased for both mRNA and protein. KRAS downstream target proteins, ERK and AKT, were downregulated as well. Furthermore, it was confirmed that DOX could be gradually released from MAH, with approximately 95% released over 72 h. Treating cells with Dox-MAH resulted in the inhibition of cell proliferation and induction of apoptosis. The protein expression of procaspase-3 and Bcl-2 was decreased, while Bax was increased, confirming that Dox-MAH triggered the cell apoptosis. The success of this research proposed a new strategy for a drug delivery system, which has multiple functions simultaneously; CRC cell-specificity, Dox carrier, and miR-143 delivery.

Keywords AS1411 aptamer, Colorectal cancer, Drug carrier, MicroRNA-143

According to GLOBOCAN 2020 data, CRC ranks as the third most common cancer worldwide and is the second leading cause of cancer deaths. It is the third most prevalent cancer among men and the second most common among women[1]. As of 2024, the treatment regimens for colorectal cancer (CRC) are tailored based on the disease stage, tumor location, and individual patient factors. These treatments typically include surgery, chemotherapy, radiation therapy, targeted therapy, and immunotherapy. Surgery is the most effective approach when the tumor is localized. In some cases, preoperative chemotherapy and radiotherapy can support the surgical procedure. Post-operative adjuvant chemotherapy is routinely administered to patients with stage III colon cancer. This treatment is given after surgery to help eliminate any remaining cancer cells and reduce the risk of recurrence. For stage II colon cancer, the decision to use adjuvant chemotherapy depends on various factors, including the risk of recurrence and the patient's overall health, and is not universally applied[2]. However, chemotherapy has several limitations, such as unwanted side effects, changes in tumor characteristics and heterogeneity within tumors, resistance to drugs, and high expenses[3]. Therefore, minimizing drug-related adverse effects is essential to enhancing chemotherapy's clinical results. Smart Drug Delivery Systems (SDDSs) were created to circumvent these limitations by conveying molecular compounds directly to target cells. SDDS has several more potential applications and can be evolved into intelligent systems. Targeted therapy is a type of cancer treatment that targets proteins involved in tumor growth and progression, i.e., molecular targets (receptors, kinase cascades, growth factors, or molecules involved in angiogenesis and apoptosis) that are overexpressed or mutated in

[1]Division of Biochemistry, Department of Preclinical Science, Faculty of Medicine, Thammasat University, Pathumthani 12120, Thailand. [2]Department of Chemistry, Faculty of Science and Technology, Thammasat University, Pathumthani 12120, Thailand. [3]Thammasat University Research Unit in Innovation of Molecular Hybrid for Biomedical Application, Pathumthani, Thailand. ✉email: pichrotk@tu.ac.th

cancer. The main objective is to selectively deliver chemotherapeutic drugs to cancer cells while minimizing the death of normal cells and preventing adverse effects[4–6].

Aptamers are short single-stranded DNA or RNA molecules known for their high binding affinity to specific targets. Typically ranging from 20 to 80 nucleotides, aptamers adopt various secondary structures such as stem-loops and G-quadruplexes. Aptamer structures are composed of a variety of secondary motifs, including stem-loop, hairpin, pseudoknot, kissing loop, three-way junction, G-quadruplex, and internal bulge structures[7]. Aptamers are robust molecules capable of withstanding high temperatures and harsh acidic or basic environments[8]. Due to their small size, they can be internalized by cells and chemically altered. Additionally, aptamers are relatively not harmful since nucleic acids are not recognized by the human immune system[9]. Aptamers can specifically bind to the targets ranging from small molecules to complex structures, making them suitable for many diagnostic and therapeutic applications[10,11]. For example, the targeted medication delivery to cancer cells is made possible by the AS1411 aptamer, which binds to the nucleolin receptor that is overexpressed in cancer cells including CRC[12,13].

Cancer is a genetic disease, meaning it arises from abnormalities in the genes that control cell behavior, especially those governing cell growth and division. KRAS mutations are observed in various malignancies and are major controlling genes. The RAS gene family KRAS, HRAS, and NRAS genes have frequently mutated in cancer, approximately 85% of all RAS mutations are KRAS mutations[14,15]. KRAS mutations are found in 50% of CRC[16,17]. Consequently, KRAS inhibitors have received a significant amount of research, as KRAS is a key target in the development of cancer therapies. It is well-known to be targeted by microRNA-143 (miR-143) and overexpression of miR-143 shows potential in inhibiting the growth of CRC cells[18].

MicroRNAs (miRNAs) or short non-coding RNAs (ncRNAs) are endogenous RNA molecules of 19–25 nucleotides in length that regulate gene expression mostly through translational inhibition or degradation of messenger RNAs (mRNA). They control the expression of genes related to cell differentiation, proliferation, and apoptosis[19–21]. One miRNA can have several impacts by binding to target mRNAs and regulating the translation of numerous proteins. A few studies have shown that altered expression of specific miRNAs has a role in the initiation and evolution of CRC[22,23]. There is also evidence that miRNAs can act as tumor suppressors or oncogenes depending on the cellular environment in which they are expressed. The miR-143 is known to act as a tumor suppressor, with many targets recognized in CRC such as MACC1, TLR2, KLF5, KRAS, AKT, ERK and Bcl2[21–25]. When compared to its level in normal tissues, the expression of mature miR-143 is typically downregulated in about 80% of human colorectal tumor samples from cancer and adenoma patients[26]. Therefore, up-regulation of miR-143 is supposed to give benefits to CRC patients because they can effectively reduce oncogene expression.

Dox is commonly called Adriamycin in the pharmaceutical industry. This agent contains planar aromatic or heteroaromatic ring systems that, after binding to sugar, sits in the minor groove by using hydrogen bonding and Van der Waals contacts to interact with flanking base pairs in the intercalation site. The planar systems slide between layers of nucleic acid pairs, disrupting the helix DNA's structure[27,28]. Dox can intercalate into genetic material mostly at GC-rich sites, inhibiting the advancement of topoisomerase II, it has broken the DNA chain for replication, blocking the release of the DNA double helix and therefore ending the replication process[29]. Currently, the chemotherapy drug Dox is used in combination with other drugs to treat cancer, such as Dox and Cisplatin in combination with FOLFOX chemotherapy treatment for gastric cancer patients[30]. Furthermore, Dox is more successful in treating advanced leiomyosarcoma when combined with Dacarbazine than used alone[31]. Although Dox has been used for decades and its efficacy and safety have been well established, it has considerable side effects, including nausea, vomiting, diarrhea, weight loss, leucopenia, irreversible cardiotoxicity, and other conditions[32,33]. To maximize therapy efficiency and avoid adverse effects, targeted drug delivery to cancer cells is a potential strategy for reducing adverse effects. Therefore, due to the intercalating properties of Dox, it can be inserted into the DNA/RNA strands. That might reduce the side effects of Dox and create a targeted delivery model for other drugs that have the same intercalating properties.

In this study, SDDS was developed, which typically consists of three major components: anticancer drugs, drug carriers, and ligands on the target tumors that can be conjugated to carriers. This research aims to develop a new hybrid complex called Dox-MAH composed of Dox and miR-143 as anticancer drugs, and AS1411 aptamer and hybridization strand (HBS) as drug carriers. The nucleolin receptor acts as a ligand on CRC cells. MiR-143, AS1411 aptamer, and HBS were combined via oligonucleotide hybridization, and subsequently loaded with Dox. Dox interacts with DNA/RNA via intercalating between the planar base pairs of duplex DNA/RNA. The AS1411 aptamer acted as a signaling molecule that specifically binds to the nucleolin receptors overexpressed on SW480 CRC cells[34,35]. The complex was then proposed to be endocytosed, with Dox and miR-143 eventually released within the cells (Fig. 1). The uptake of Dox-MAH into SW480 cells was verified by measuring fluorescence intensity of FAM-labelled AS1411. Upon the treatment of MAH, the expression levels of miR-143, KRAS, and its downstream target proteins, ERK and AKT were investigated using RT-PCR and western blot analysis. Additionally, the effects of Dox-MAH on cell proliferation and apoptosis were explored. This research demonstrates a novel approach for an SDDS that combines CRC cell targeting and delivery of Dox and miR-143 in one solution.

Materials and methods

Sequence design for aptamers, miR-143, and a hybridization strand

To establish a hybridization site for the miR-143 and AS1411 aptamer, additional oligonucleotides completely compatible with the hybridization strand (HBS) were extended at the 3′ end. Furthermore, hybridization strands were designed to complement those specific regions. miR-143 was modified with a 2′-*O*-Methylation (2′OMe) at two positions: at the naturally modified position and the 3′ end, to enhance stability and prevent degradation before entering the cell. The sequence of HBS was complementary to the additional oligonucleotides of the aptamer and miR-143. Hybridization between these sequences was computationally tested using the Oligo

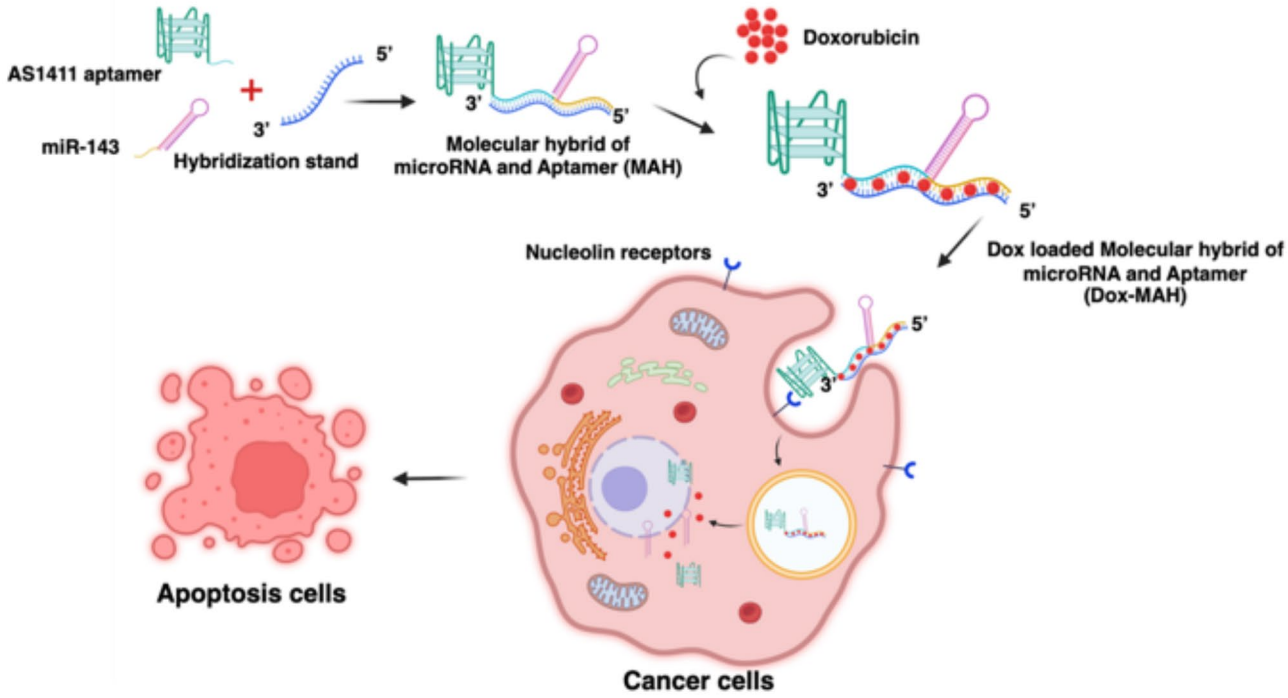

Fig. 1. Structure sketch of Dox-MAH, consisting of Dox, miR-143, AS1411 aptamer, and HBS. When AS1411 aptamer binds to the nucleolin receptor on CRC cells, Dox-MAH is taken up, and then Dox and miR-143 are released into the cells.

Name	Modification	Sequence 5′→3′
miR-143	2′-*O*-Methylation	5′-UGAGAUGAAGCACUGUAGCUC CCTGACTTGAGCAAAATTGACT-3′
AS1411 aptamer	–	5′-GGTGGTGGTGGTTGTGGTGGTGGTGG CCATCGGCTATCGAAGCTCGAT-3′
Non-specific aptamer	–	5′-TTCCTCCTCCTCCTTCTCCTCCTCCTCC ATCGGCTATCGAAGCTCGAT-3′
Hybridization stand (HBS)	–	5′-TCCAGTTTTAAGTCAATTTTGCTCAAGTCAC ACCCCGCTAATCGAGCTTCGATAGCCGAT-3′

Table 1. List of nucleotides with modifications highlighted in red. The underline indicates the original sequences.

Analyzer tool (Integrated DNA Technologies, IDT, USA), and the sequences were summarized in Table 1. All oligonucleotides were purchased from IDT, USA.

Study of formation and in vitro stability of MAH using gel electrophoresis

To prepare the MAH, miR-143, AS1411 aptamer, and a hybridization strand were combined at a final concentration of 1 μM each. The mixture was incubated at room temperature for 48 h to allow MAH formation via intermolecular hybridization. The hybridization products were confirmed using 10% native polyacrylamide gel electrophoresis. To check the stability of the MAH, miR-143, AS1411 aptamer, and the hybridization strand were mixed at a final concentration of 1 μM in Dulbecco's Modified Eagle's Medium (DMEM) and incubated at 37 °C in a 5% CO_2 atmosphere for 1–7 days. The stability of the MAH was evaluated using 10% native polyacrylamide gel electrophoresis.

Cell culture

A human colorectal adenocarcinoma cell line (SW480 and Caco-2) and a normal colon epithelial cell line (CCD 841 CoN) were obtained from the American Type Culture Collection (ATCC, USA). The cells were cultured in DMEM (Gibco, USA) containing 10% fetal bovine serum (FBS) (Gibco, USA) and 1% penicillin-streptomycin (Gibco, USA) at 37 °C in a 5% CO_2 atmosphere. Upon reaching 80% confluence, the cells were subcultured using 0.05% trypsin in phosphate-buffered saline (PBS).

Cellular uptake analysis using a fluorescence microscope

Approximately 3×10^4 SW480 and CCD 841 CoN cells were seeded into each well of 96-well plates and incubated for 24 h at 37 °C in a 5% CO_2 atmosphere. The media were then removed, and the cells were treated with either MAH or a complex of miR-143, a non-specific aptamer, and HBS, referred to as MNH, at a concentration of 10 µM in a final volume of 100 µL DMEM for 1 h. Non-treated cells served as a control. Following treatment, the nuclei were stained with 100 µL of 4′,6′-diamidino-2-phenylindole dihydrochloride (DAPI) solution (Sigma-Aldrich, USA) for 10 min. The cells were then washed with PBS. Finally, cells were observed and imaged using an ECLIPSE Ts2R inverted fluorescence microscope (Nikon, USA). The binding capacity of MAH and MNH to SW480 and CCD 841 CoN cells was assessed. For microscopic visualization, green-emitting fluorescein (FAM) was conjugated to the 5′ end of the AS1411 aptamer and the non-specific aptamer. The 5′ 6-FAM-modified oligonucleotides were purchased from IDT, USA.

Treatment of MAH and MNH in SW480 cells

Approximately 1×10^5 cells of SW480 were seeded into each well of 24-well plates and further incubated for 24 h at 37 °C, 5% CO_2 atmosphere. Next, the media was removed, and the cells were treated with MAH and MNH at concentrations of 10 µM in a final volume of 400 µL DMEM for 48 h at 37 °C, 5% CO_2 atmosphere, and non-treated cells served as a control. After that, cells were washed with 500 µL PBS twice, added with 200 µL of 0.05% trypsin-EDTA, and incubated for 5 min at 37 °C, 5% CO_2 atmosphere. Then, 400 µL DMEM was added, and all the substances were transferred to a 1.5 mL tube and centrifuged at 1000 rpm for 5 min. After that, cells were washed again with 500 µL PBS twice and subjected to the total RNA extraction.

Quantification of miR-143 and *KRAS* mRNA levels by quantitative RT-PCR

Total RNA was extracted from conditioned cells (SW480, Caco-2, and CCD 841 CoN) using the miRNeasy Micro Kit (Qiagen, USA) according to the manufacturer's protocol. The mature miR-143 levels were assessed using TaqMan microRNA Assays (Applied Biosystems, USA) with the Mastercycler nexus Gradient (Eppendorf, Germany). Briefly, 10 µg of total RNA was reverse-transcribed to cDNA using a TaqMan™ microRNA reverse transcription kit (Applied Biosystems, USA), and the expression of miR-143 was measured by qPCR. The sequences of the primers (Applied Biosystems, USA) were as follows: human U6 forward primer: 5′-CGCTTCA CGAATTTGCGTGTCA-3′ and human U6 reverse primer: 5′-GCTTCGGCAGCACATATACTAAAAT-3′. The reaction conditions were as follows: 95 °C for 10 min, followed by 40 cycles at 95 °C for 15 s and 60 °C for 60 s. U6 small nuclear RNA was used for normalization of miRNA.

For the evaluation of *KRAS* mRNA levels, 10 µg of total RNA was reverse-transcribed to cDNA using High Capacity cDNA Reverse Transcription Kits (Applied Biosystems, USA). The reaction conditions were 25 °C for 10 min, 37 °C for 120 min, and 85 °C for 5 min. Quantification of *KRAS* and *GAPDH* transcripts was performed by real-time PCR using TaqMan Gene Expression Assays with FAM-conjugated MGB (minor groove binder) probes: *KRAS* (cat# Hs00364282_m1) and *GAPDH* (cat# Hs99999905_m1). The reactions were incubated at 95 °C for 10 min, followed by 40 cycles of 95 °C for 15 s and 60 °C for 60 s. The relative expression levels of miR-143, *KRAS*, and *GAPDH* mRNA were calculated using the $2^{-\Delta\Delta Ct}$ method.

Western blot analysis

The 3×10^5 SW480 cells treated under various conditions were collected after 72 h. The cell pellets were washed three times with cold PBS, lysed with RIPA buffer (Ameresco, USA) containing protease inhibitors (Ameresco, USA), and sonicated until completely dissolved. Protein concentration was measured using a Pierce BCA Protein Assay Kit (Thermo Scientific, USA). The 40 µg of protein samples were subjected to polyacrylamide gel electrophoresis (PAGE) using a 12% resolving gel and a 4% stacking gel, and then transferred to a PVDF membrane by electroblotting. After blocking with Odyssey Blocking Buffer for 1 h at room temperature, the membranes were incubated with primary antibodies overnight at 4 °C. The primary antibodies used were: KRAS (Cat #703345, Thermo Scientific, USA), ERK (Cat #9102), Akt (Cat #9272), procaspase-3 (Cat #9662), Bax (Cat #2772), Bcl-2 (Cat #4223), α-tubulin (internal control, Cat# 2144) (Cell Signaling Technology, USA). Following this, the membranes were incubated with the secondary antibody at room temperature for 1 h. Band visualization and quantification were performed using a LI-COR Odyssey Imager (Li-COR, USA).

Investigation of Dox intercalation into MAH by fluorescence spectroscopy

The successful intercalation of Dox into the CG site of oligonucleotide duplexes is important for the preparation of Dox-MAH molecules. Dox, at a final concentration of 0.95 µM, was mixed with 5 µM of MAH in pH 7.4 PBS for 1.5 h at room temperature. The fluorescence spectra of Dox and Dox-MAH were then measured using a Varioskan LUX microplate reader (Thermo Scientific, USA) with an excitation wavelength of 480 nm and an emission wavelength range of 500–800 nm.

Dox release studies

To simulate the release of Dox within cells, Dox-MAH was transferred into conditioned DMEM media that had been used to culture SW480 cells for 48 h and contained various nucleases[36]. The Dox-containing media were collected at 1, 3, 6, 12, 24, 48, and 72-h intervals, and the absorbance of Dox was measured using a UV–Vis spectrophotometer at 480 nm. The quantity of released Dox was determined using a standard curve of Dox in the conditioned media. The percentage of cumulative Dox release was calculated using the following equation: Cumulative drug release (%) = $(A_T/A_D) \times 100\%$, where A_T is the amount of drug released at a given time and A_D is the total amount of drug.

Cell proliferation assay

To study the effects of Dox-MAH on CRC and normal colon cell proliferation, SW480 and CCD 841 CoN cells were seeded into 96-well plates at 5×10^3 cells per well in DMEM and incubated for 24 h at 37 °C in a 5% CO_2 atmosphere. Before treatment, the formulations of Dox-MAH and Dox-MNH were freshly prepared to achieve a final concentration of 5 μM by mixing Dox with MAH or MNH in DMEM for 1.5 h at room temperature. The media were removed from the cells, which were then treated with MAH, MNH, Dox, Dox-MAH, and Dox-MNH at concentrations of 5 μM for the complexes and 0.95 μM for Dox, in a final volume of 100 μL of DMEM. Non-treated cells served as controls. Cell viability was determined by adding 20 μL of MTS solution (Promega, USA) to each well and incubating at 37 °C for 1 h. Absorbance was then measured at 490 nm using a Multiskan FC microplate reader (Thermo Scientific, USA). The percentage of cell viability was calculated using the following equation: Percentage of cell viability = $(A_{test} - A_{blank})/(A_{control} - A_{blank}) \times 100\%$. Here, A_{test} is the absorbance of the treated cells, $A_{control}$ is the absorbance of untreated cells, and A_{blank} is the absorbance of the MTS solution without cells.

Apoptosis detection using flow cytometry analysis

SW480 cells (3×10^5) were treated with 0.54 μM Dox, 5 μM Dox-MAH, and 5 μM Dox-MNH for 48 h. After treatment, the cells were washed twice with PBS and incubated with the FITC Annexin V/propidium iodide (PI) apoptosis detection reagent for 15 min at room temperature. The samples were then analyzed using a flow cytometer to assess apoptosis. FITC Annexin V binds to phosphatidylserine molecules that have translocated to the outer leaflet of the plasma membrane, marking early apoptotic cells. PI, a DNA-binding dye, penetrates cells with compromised membranes, labeling the DNA of late apoptotic and necrotic cells. This dual staining approach distinguishes between viable, early apoptotic, late apoptotic, and necrotic cells.

Statistical analysis

All data are presented as the mean ± standard deviation (SD) of at least triplicate samples. Comparisons between the control and study groups were performed using one-way analysis of variance (ANOVA) followed by Dunnett's T3 test. Statistical significance was defined as $P < 0.05$.

Results

Formation and in vitro stability of MAH

To test the successful formation and stability of MAH, the products were examined using 10% native polyacrylamide gel electrophoresis. A distinct band corresponding to the size of MAH (151 bp) was observed (Fig. 2A). MAH was successfully formed via the intermolecular hybridization of the oligonucleotide sequences. Subsequently, to verify MAH's stability, its integrity was monitored over a period of 1–7 days. The results showed that MAH was extremely stable, as the bands remained visible even on day 7. Additionally, the amount of MAH slightly increased from day 1 to day 7, suggesting that a longer incubation time might result in a greater number of products (Fig. 2B).

Expression of miR-143 in CRC and normal colon cell lines

To compare miR-143 expression levels between CRC and normal colon cells, we investigated two human colorectal adenocarcinoma cell lines (SW480 and Caco-2) and a normal colon epithelial cell line (CCD 841 CoN). The expression levels of miR-143 were dramatically downregulated in both SW480 and Caco-2 cells compared to those in normal cells. However, the miR-143 level in SW480 cells was much lower than that in Caco-2 cells, so they were used in the subsequent investigations (Fig. 3). This result also confirmed that miR-143 was significantly underexpressed in CRC cells, suggesting that increasing miR-143 levels might be a promising strategy for combating CRC cells.

In vitro cellular uptake of MAH

MAH binding capability

The aptamers were tagged with FAM, a green fluorophore, to investigate the cellular uptake and binding capabilities of MAH. FAM-tagged MAH and MNH were used exclusively for fluorescence imaging to study their interactions with cells and were not used for other experiments. To evaluate the binding specificity, SW480 cells and normal CCD 841 CoN cells were treated with FAM-tagged MAH and MNH, and examined using a fluorescence microscope. The results demonstrated that SW480 cells treated with MAH produced a significantly higher fluorescence signal compared to cells treated with MNH and untreated controls (Fig. 4A). This suggests that the AS1411 aptamer in MAH binds specifically to SW480 cells via interactions with nucleolin receptors on the cell surface. In contrast, when CCD 841 CoN cells were examined, neither MAH nor MNH treatment resulted in changes in fluorescence intensity under the FAM channel of the microscope (Fig. 4B). These findings indicate that the hybrid molecule MAH exhibits higher specificity toward cancer cells than normal cells.

Expression of exogenous miR-143

To determine whether MAH effectively delivers miR-143 into SW480 cells, we examined the levels of miR-143 in the cells treated with MAH and MNH. The results showed that miR-143 expression was 4-fold higher in SW480 cells treated with MAH compared to those treated with MNH or untreated (Fig. 5A). These findings demonstrate that the AS1411 aptamer facilitates the delivery of MAH molecules carrying miR-143 specifically to cancer cells, resulting in elevated miR-143 expression.

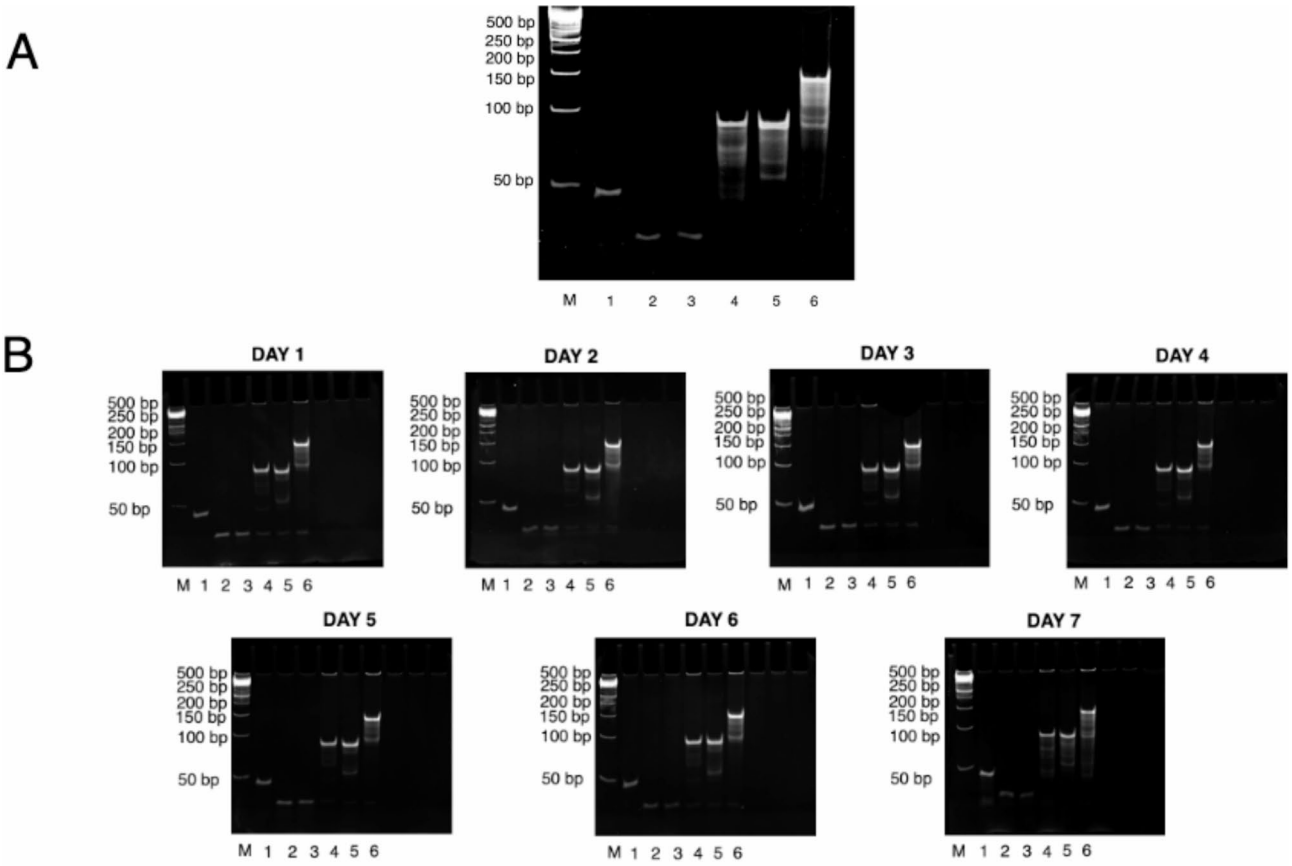

Fig. 2. (**A**) Formation of MAH investigated by 10% polyacrylamide gel electrophoresis. Lane M: 1 kb DNA ladder, Lane 1: HBS, 60 bp, Lane 2: AS1411 aptamer, 48 bp, Lane 3: miR-143, 43 bp, Lane 4: HBS and AS1411 aptamer: 108 bp, Lane 5: HBS and miR-143, 103 bp, and Lane 6: HBS, AS1411 aptamer, and miR-143 (MAH), 151 bp. (**B**) Gel electrophoresis was utilized to confirm the in vitro stability of MAH on day 1–day 7. Lane 6 indicates the intact bands of MAH.

Investigation of alteration of miR-143 target gene products

Effects of miR-143 on KRAS mRNA and protein expression

Since KRAS is a direct target of miR-143, we assessed KRAS mRNA and protein levels in cells treated with MAH and MNH using RT-qPCR and Western blot analysis, respectively. The results demonstrated a 0.5-fold decrease in KRAS mRNA (Fig. 5B) and a 0.5-fold reduction in protein levels (Fig. 5C) in cells treated with MAH compared to those in untreated cells. This finding confirms that MAH treatment led to miR-143 overexpression and subsequent down-regulation of KRAS expression at both mRNA and protein levels.

Effects of miR-143 on AKT and ERK protein levels

The activated KRAS protein can trigger various signaling pathways, such as the RAF-MEK-ERK pathway, PI3K-AKT-mTOR pathway, and other signaling pathways[37]. To further confirm whether the KRAS function is blocked by miR-143, KRAS downstream target proteins, AKT and ERK, were analyzed in MAH-treated SW480 cells. Consistent with the results for KRAS expression, SW480 cells treated with MAH exhibited significantly reduced levels of ERK (≈ 0.6-fold) and AKT (≈ 0.6-fold) proteins compared to untreated cells (Fig. 5C). These findings suggest that miR-143 effectively disrupts the KRAS signaling network.

Intercalation of Dox into MAH

Dox was incorporated into MAH due to its ability to intercalate into DNA duplexes. Fluorescence quenching of Dox resulting from its integration into MAH was observed. The fluorescence spectrum showed that Dox alone (represented by the green line) has a peak fluorescence emission at approximately 590 nm. Upon complexation with MAH, this fluorescence was significantly suppressed, as indicated by the yellow line, demonstrating successful intercalation (Fig. 6A). This result confirms that Dox effectively incorporates into the MAH molecule, with the intercalation primarily driven by interactions between Dox's aromatic moiety and the GC base pairs in the molecular hybrid.

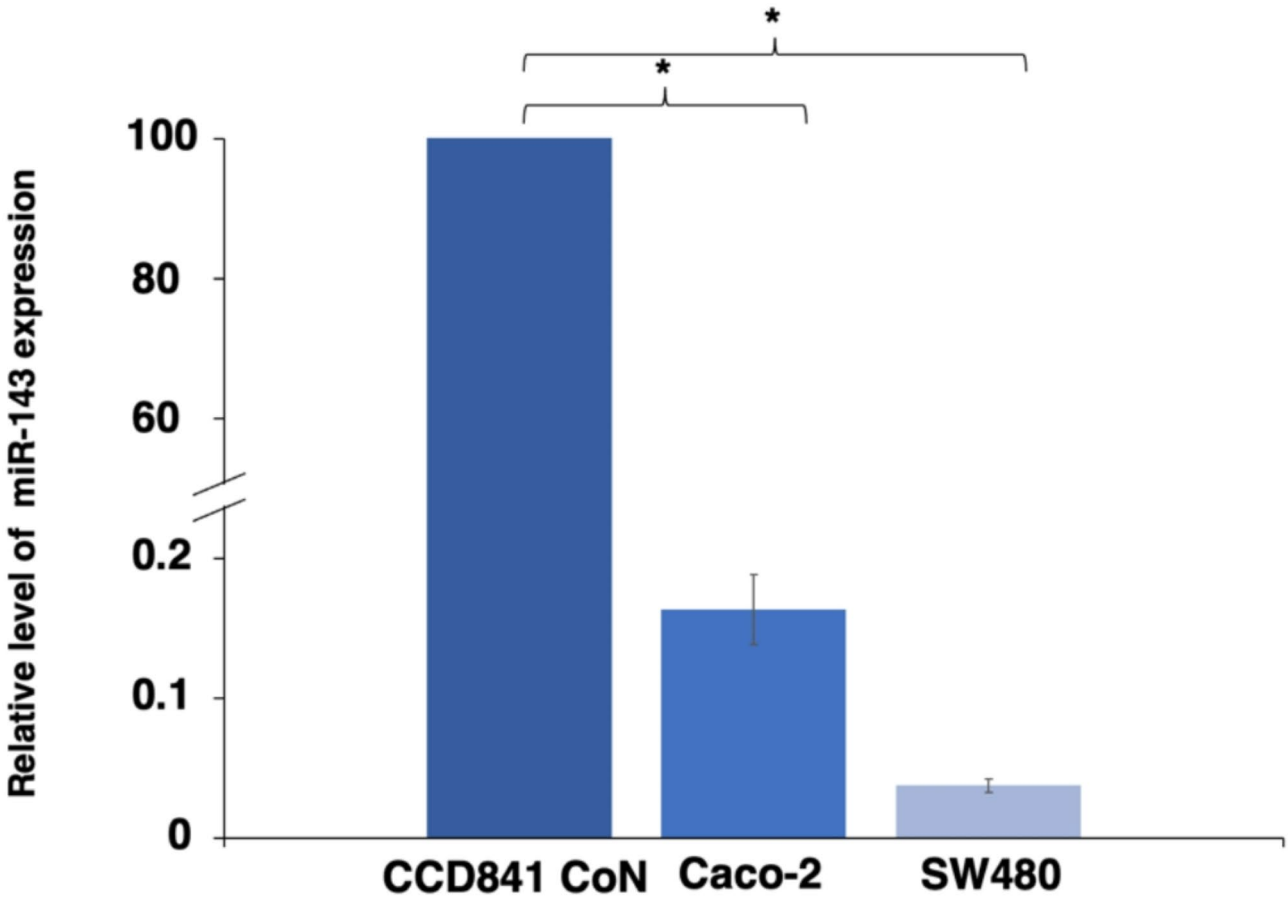

Fig. 3. MiR-143 expression was dramatically down-regulated in Caco-2 and SW480 cells, compared to CCD 841 CoN using RT-qPCR analysis.

In vitro Dox release

After confirming the intercalation of Dox into MAH, the cumulative release of Dox from MAH was studied. Dox was gradually released from MAH, starting at around 5% at 1 h and reaching approximately 80% at 48 h (Fig. 6B). These results suggest that MAH exhibited efficient sealing properties, which can prolong Dox release and improve Dox retention in SW480 cells. Furthermore, when SW480 cells were treated with Dox-MAH and Dox, even at 1 h, the absorbance of Dox in the media at 480 nm was very low and not significantly different from that in untreated cells, which served as the control (Supplementary Fig. 2). These results imply that free Dox passively diffused into cells as early as the first hour and that Dox-MAH was successfully internalized into cells, consistent with the increase in miR-143 observed after MAH treatment in the previous experiment. Taken together, these findings suggest that MAH enhances the specific targeting, internalization, and prolonged release of Dox, thereby increasing its safety and efficacy.

Effects of Dox-MAH on the SW480 and CCD 841 CoN cell proliferation

We further investigated the potential anti-proliferative effects of Dox-MAH in both normal and cancer cells. SW480 cells were treated with MAH, MNH, Dox-MAH, Dox-MNH, and Dox at the IC50 concentration of Dox (0.95 μM), with untreated cells serving as controls. Cytotoxicity was determined at 48 h using the MTS assay. The results showed that Dox-MAH effectively inhibited the proliferation of SW480 cells, with its efficacy comparable to that of Dox alone (Fig. 6C). Both Dox-MAH and Dox exhibited similar growth suppression capabilities. Additionally, SW480 cells treated with Dox-MAH had lower cell viability compared to those treated with MAH alone, suggesting that Dox contributes to increased toxicity. Cells treated with Dox-MNH showed less harm, indicating that the AS1411 aptamer enhances the efficacy of Dox. This study highlights that the AS1411 aptamer, serving as a recognition and uptake facilitator, modulates Dox toxicity. To further assess the effect of Dox-MAH on normal colon cells, CCD 841 CoN, cell viability results are shown in Fig. 6D. The data revealed that the treatment molecules were not harmful to normal colon cells. Therefore, Dox-MAH efficiently suppressed the growth of SW480 cancer cells while exerting minimal effects on normal colon cells.

Detection of CRC cell apoptosis after Dox-MAH treatment

To further investigate whether Dox-MAH triggers apoptosis, SW480 cells were treated with Dox-MNH, Dox-MAH, and Dox for 48 h. Flow cytometry with Annexin V-FITC/PI double staining was used to assess apoptotic

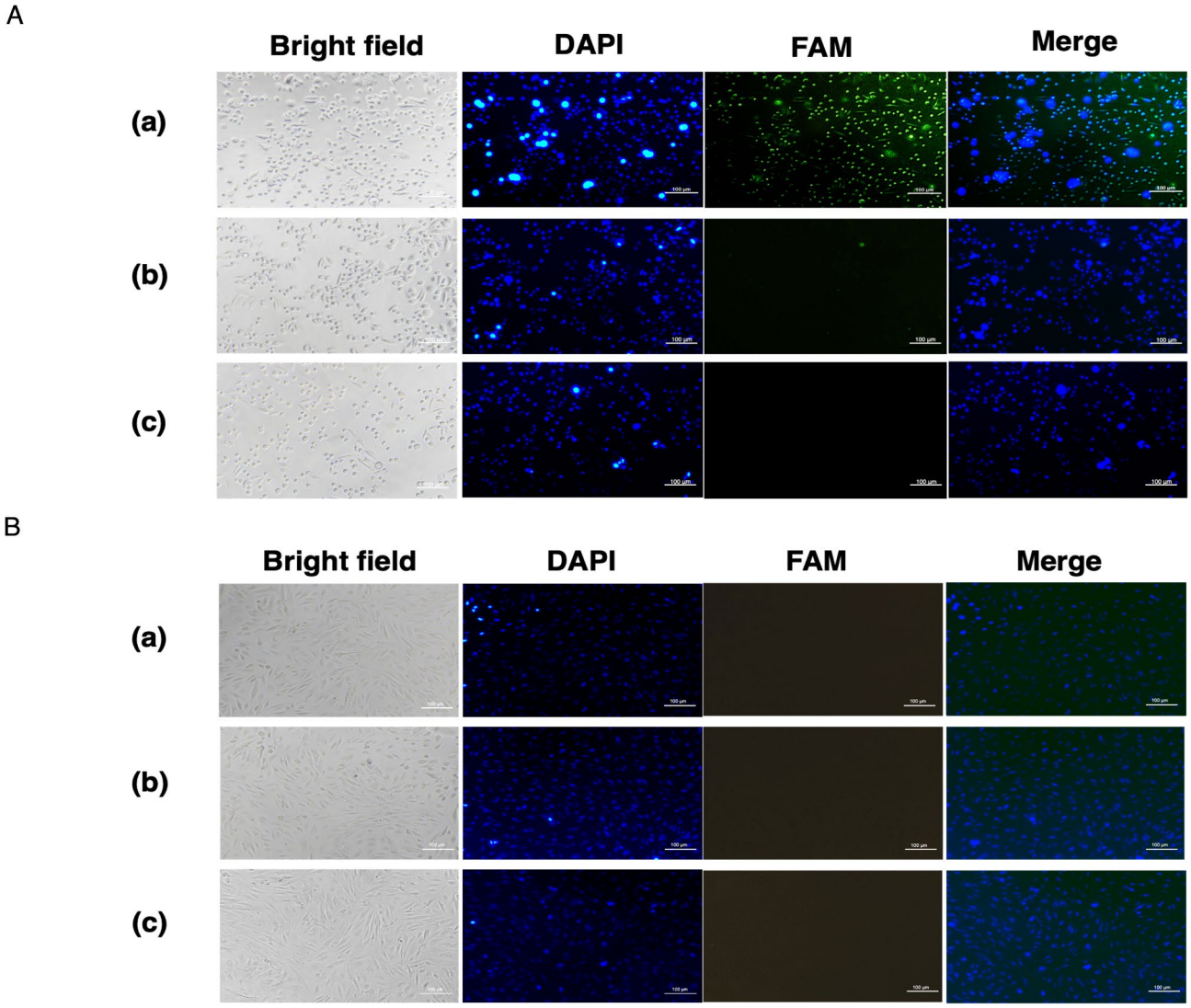

Fig. 4. (**A**) Fluorescent image of SW480 treated with 10 μM MAH (a), 10 μM MNH (b), and untreated (c). (**B**) Fluorescent image of CCD 841 CoN treated with 10 μM MAH (a), 10 μM MNH (b), and untreated (c). The AS1411 and non-specific aptamers were labeled with FAM. (Scale bar: 100 μm)

cells. However, the emission spectrum of Dox overlaps with that of PI, which is commonly used to stain dead cells. To minimize interference from Dox fluorescence in the analysis, the concentration of Dox was reduced to 0.54 μM, while still remaining within the cytotoxic concentration range. Flow cytometric data indicated a significant reduction in the percentage of viable cells in the SW480 cells treated with Dox-MAH (Fig. 7A). To quantify apoptosis, the percentage of apoptotic cells was calculated by summing the proportions of early and late apoptotic cells. These percentages were 5.49 ± 0.21%, 9.75 ± 0.53%, 13.59 ± 1.03%, and 16.36 ± 2.80% in the control, cells treated with Dox-MNH, Dox-MAH, and Dox, respectively (Fig. 7B). Dox-MAH induced apoptosis at a rate comparable to that induced by Dox alone. In contrast, cells treated with Dox-MNH exhibited a significantly lower rate of apoptosis compared to those treated with Dox-MAH and Dox. These findings suggest that Dox-MAH can inhibit SW480 cell growth by inducing apoptosis and that the AS1411 aptamer enhances the uptake of Dox into SW480 cells.

Western blot analysis of apoptosis-related proteins

The effects of Dox-MAH on the pro-apoptotic proteins Bax and procaspase-3, as well as the anti-apoptotic protein Bcl-2, were investigated. After SW480 cells were treated for 72 h as described, Western blot analysis revealed that both Dox and Dox-MAH led to a 1.5-fold increase in Bax levels and a 0.4-fold and 0.3-fold decrease in Bcl-2 levels, respectively (Fig. 7C). This shift resulted in a higher ratio of Bax to Bcl-2 proteins, which is associated with alterations in mitochondrial membrane permeability and structure.

A key step in the apoptotic process is the caspase pathway, a series of cysteine proteases. Caspases are crucial for the execution of apoptosis, orchestrating the dismantling of cellular components and the progression of cell death. Notably, caspase-3 is essential for executing apoptosis. Once procaspase-3 is cleaved into caspase-3,

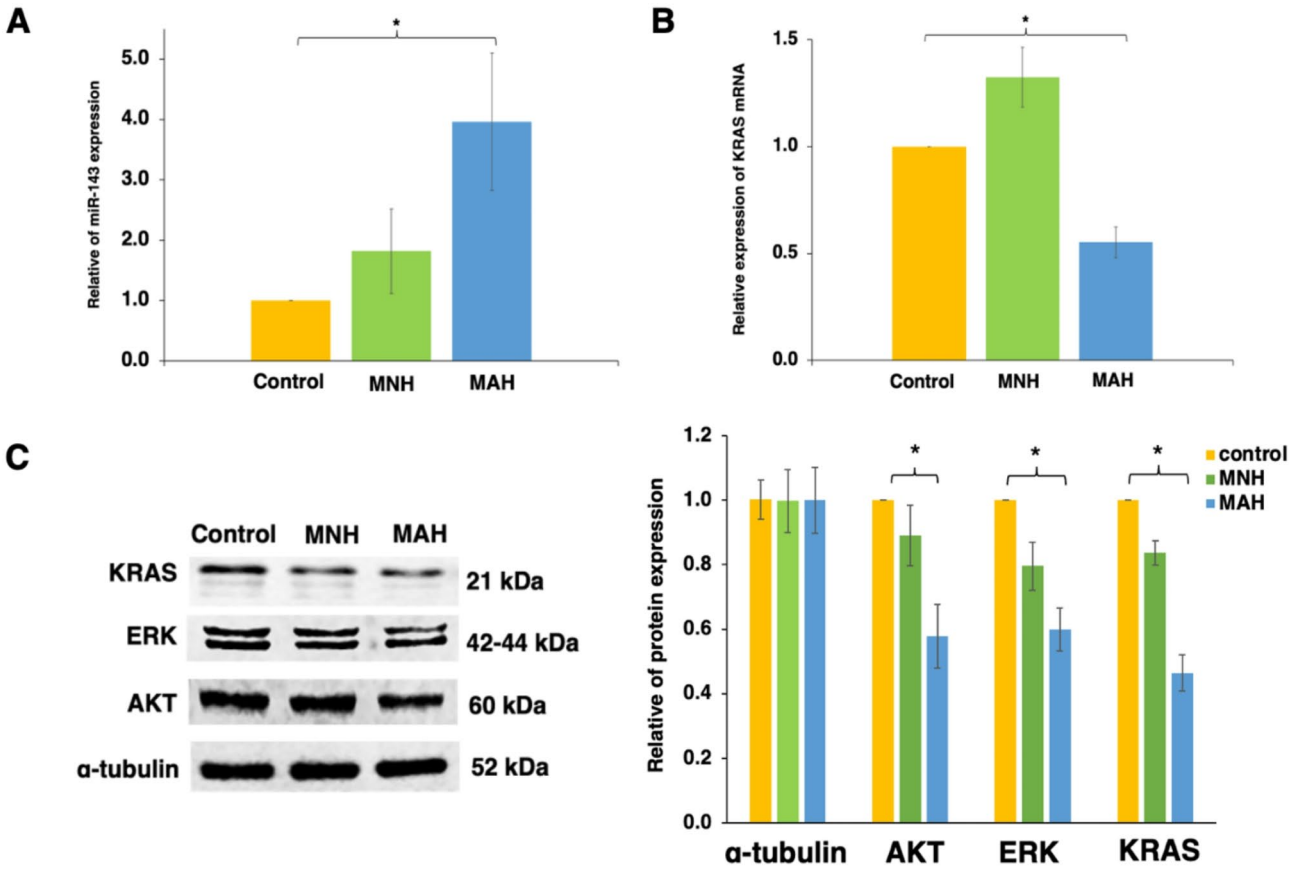

Fig. 5. After MAH treatment in SW480 cells, (**A**) miR-143 expression levels significantly increased, while (**B**) *KRAS* mRNA expression was significantly reduced. (**C**) The protein levels of KRAS, AKT, and ERK were subsequently deceased. Histograms represent quantitative analysis of band intensities normalized as to α-tubulin. The original images of blots are shown in Supplementary Fig. 1. All data were expressed as mean ± SD from triplicate experiments. $^{*}P \leq 0.05$ indicates a significant difference.

the active caspase-3 then activates numerous cellular proteins, leading to the characteristic morphological changes observed in apoptotic cells. Consequently, a significant 0.4-fold decrease in procaspase-3 levels was observed in SW480 cells treated with Dox-MAH (Fig. 7C). Taken together, these results confirm that Dox-MAH induces apoptosis, suggesting that Dox-MAH selectively targets SW480 cells and triggers cell death through the mitochondrial-dependent pathway.

Discussion

The complexity of cancer and its resistance to treatments make single-drug therapies often insufficient for effective advanced cancer treatment. Multi-target approaches, such as combination therapies and polypharmacology, offer enhanced therapeutic benefits, improved safety, and reduced resistance risk. The shift from "one drug, one target" to "network-targeted multi-component therapeutics" reflects this change[38]. Despite the success of combination therapies, challenges remain, such as interactions that affect drug ratios and efficacy and increased toxicity. Addressing these issues involves SDDSs to improve targeting and reduce side effects. Hybrid drugs, which combine multiple bioactive compounds into one molecule, represent an advanced form of combination therapy. These drugs aim to target multiple cancer pathways, potentially offering better efficacy and fewer side effects compared to traditional combination therapies[39].

Our previous study successfully established a molecular hybrid via oligonucleotide hybridization and loaded Dox into the DNA duplex. It was also confirmed that the AS1411 aptamer acted as a recognition molecule, effectively guiding the complex to CRC cells[40]. This finding motivated us to create a molecular hybrid composed of AS1411 and RNA, as non-coding RNAs (ncRNAs), such as miRNAs, have emerged as key regulators of critical growth pathways in cancer pathogenesis. Research has shown that miRNA-based therapies, whether by inhibiting oncogenes or inducing tumor suppressors, can be effective in cancer treatment[41].

This research successfully developed a molecular hybrid (MAH) combining the tumor-suppressor miR-143 and the AS1411 aptamer as an anticancer drug carrier. The MAH was created by hybridizing miR-143 with the AS1411 aptamer and loading it with the chemotherapy drug Dox within a DNA-RNA duplex. Dox-MAH leverages the advantages of three key components: the specificity of the AS1411 aptamer, the multi-oncogene targeting of miR-143, and the intercalation of Dox into nucleotides. The AS1411 aptamer specifically binds to

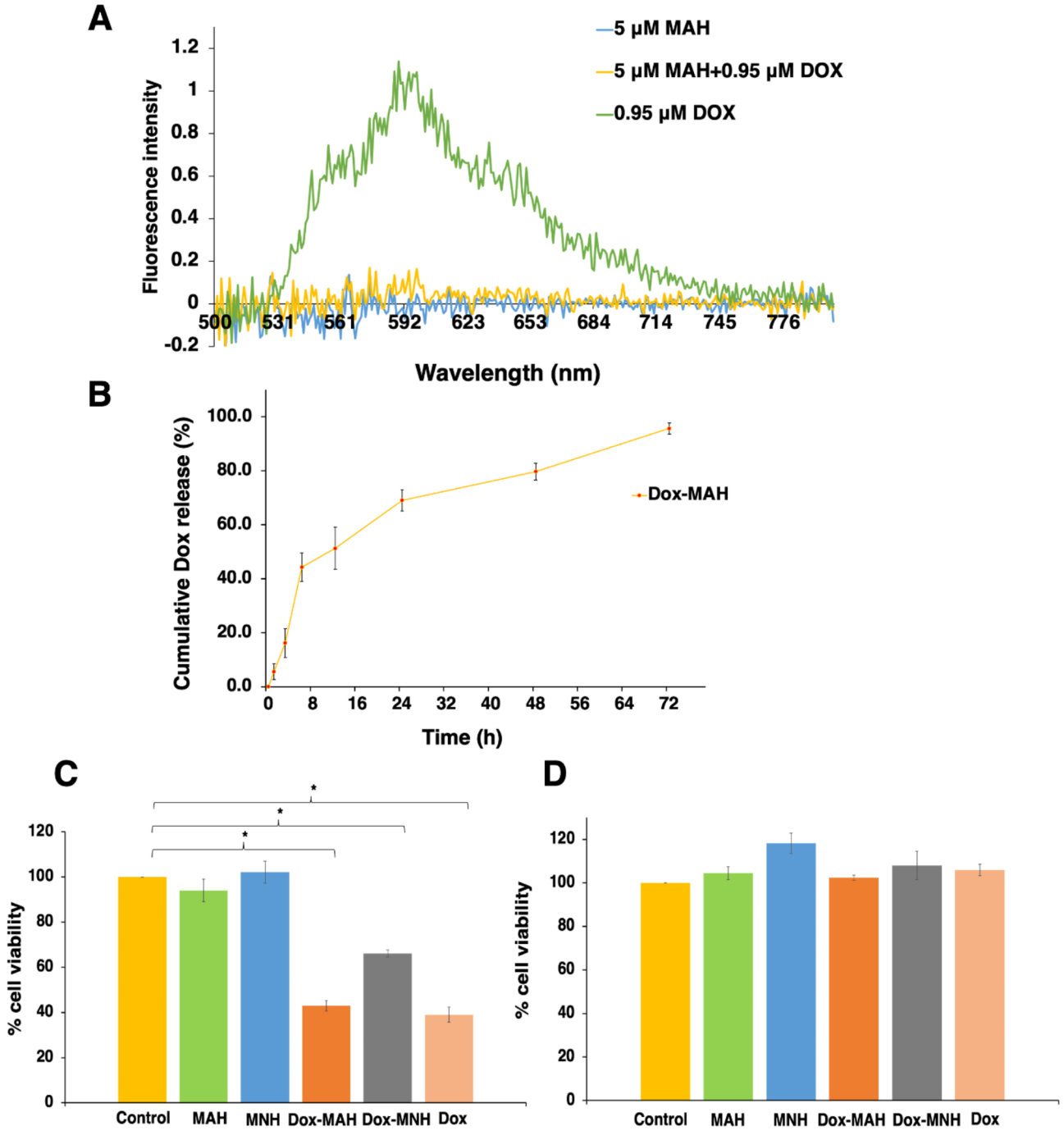

Fig. 6. (**A**) Fluorescence spectra of 0.95 μM free Dox solution (green line), 5 μM MAH (blue line), and 5 μM MAH incubated with 0.95 μM Dox for 1.5 h (yellow line). (**B**) In vitro drug release profile of Dox from MAH at 37 °C for 72 h. Dox release was monitored by measuring the absorbance at 480 nm and was expressed as a percentage, calculated as described in the text. Effects of Dox-MAH on (**C**) SW480 and (**D**) CCD 841 CoN cell proliferation are shown. Data are presented as mean ± SD, $N = 3$, $^*P < 0.05$.

nucleolin receptors on SW480 cells, facilitating the endocytosis of MAH. Given that nucleolin expression is low on normal colon cells[35], but overexpressed on many cancer types, including CRC, AS1411 aptamer selectively targets cancer cells[12,13]. This suggests that MAH could be effective against not only CRC but potentially several other cancers as well. Additionally, AS1411 exhibits anti-proliferative effects on cancer cells by upregulating p53 and downregulating Bcl-2 and Akt1 through modulation of nucleolin, which inhibits cell migration[42,43]. This enhances the anticancer efficacy of the MAH complex.

Upon treating SW480 cells with MAH, we observed a significant increase in miR-143 levels, accompanied by a marked decrease in oncogenic KRAS mRNA and protein levels, as well as reductions in the downstream target

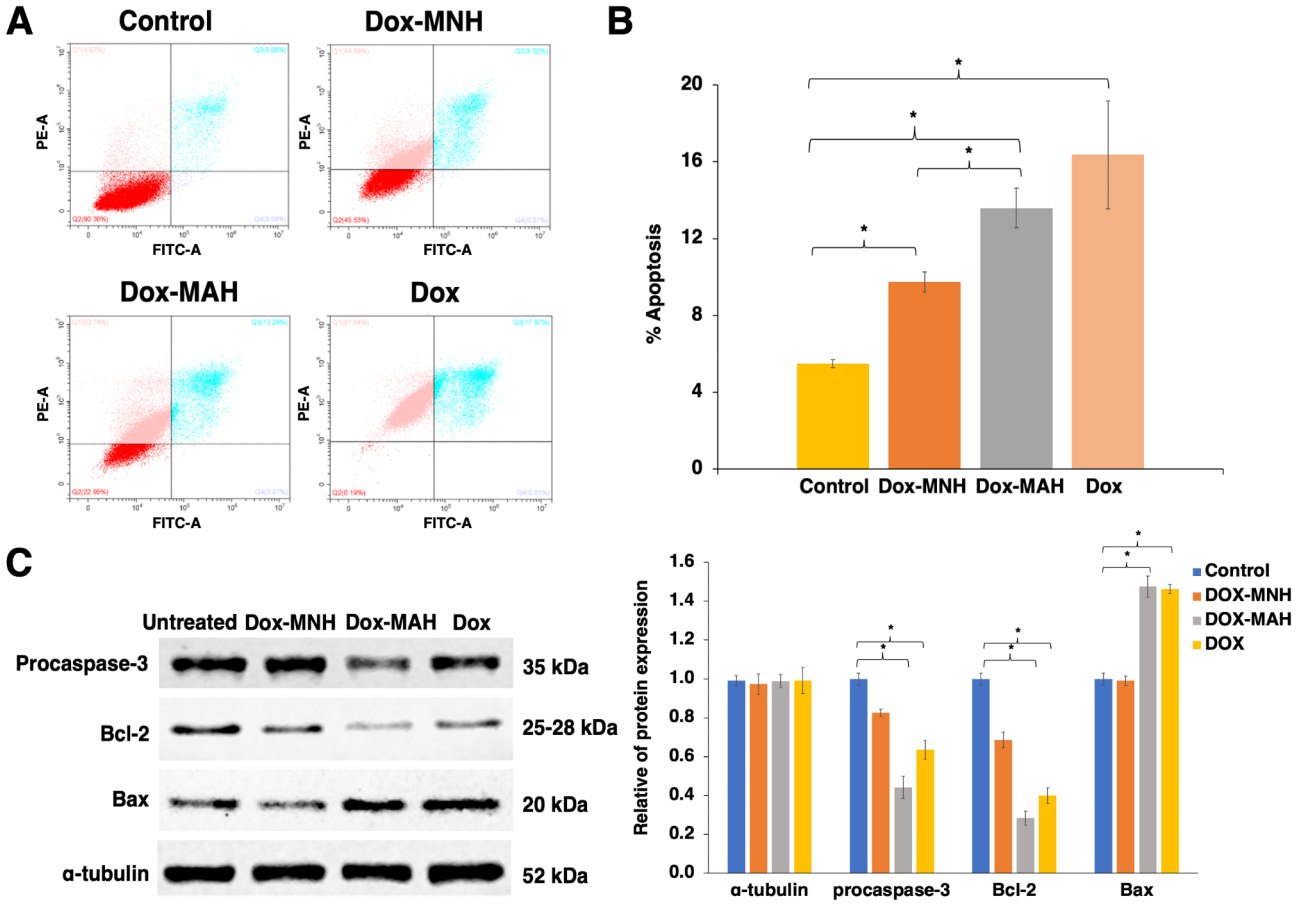

Fig. 7. (**A**) Apoptosis induction in SW480 cells by Dox-MAH was analyzed using flow cytometry. The scatter plots display the percentages of cells in each state: Q1 (necrotic cells), Q2 (live cells), Q3 (late apoptotic cells), and Q4 (early apoptotic cells). (**B**) The bar graph illustrates the percentages of apoptotic cells, including both early and late apoptosis, for each condition. (**C**) Alterations in apoptosis-related proteins in CRC cells following treatment with Dox-MNH, Dox-MAH, and Dox were assessed. Untreated cells served as controls. After exposing SW480 cells to these treatments for 72 h, cell lysates were collected for Western blot analysis using antibodies against Bcl-2, Bax, and procaspase-3. Histograms represent the quantitative analysis of band intensities, normalized to α-tubulin. The original images of blots are shown in Supplementary Fig. 3. All data are expressed as mean ± SD from triplicate experiments. $^{*}P \leq 0.05$ indicates statistical significance.

proteins AKT and ERK. KRAS is a key target of miR-143, as supported by computational predictions using tools such as TargetScan, miRanda, and PicTar, and confirmed through experimental validation[18,44]. Various strategies have been developed to inhibit KRAS signaling, targeting either upstream activators or downstream effectors of the KRAS pathway. The PI3K/PTEN/AKT and RAF/MEK/ERK pathways are critical in tumorigenesis and contribute to chemotherapy drug resistance[45]. Targeting these pathways could enhance CRC chemotherapy efficacy. The observed reduction in AKT and ERK in our study can be attributed to two mechanisms: (1) they are downstream signaling pathways of KRAS, and (2) they are also direct targets of miR-143[46] (Fig. 8). Recent research indicates that simply knocking down KRAS with KRAS siRNA is insufficient to inhibit CRC cell growth, as it does not reduce AKT and ERK protein levels[47]. In contrast, miR-143 effectively addresses this issue. Our study emphasizes the importance of targeting multiple key genes within the KRAS network using Dox-MAH. This approach is essential because KRAS mutant cancers often depend on a positive feedback loop for survival, which is activated when KRAS, AKT, and MAPK pathways do not receive adequate suppressive signals. Furthermore, other signaling pathways impacting AKT or ERKs can also activate this survival mechanism.

The downregulation of miR-143 is observed across various human malignancies[48,49]. This miRNA plays a preventive role in tumor development and regulates the expression of multiple genes, including Bcl-2, DNMT3A, ERK5, C-Myc, Bax, caspase-3, caspase-9, and ELK1, which are implicated in cell growth, survival, differentiation, and invasion[23,49–51]. MiR-143 replacement therapy could thus provide a promising therapeutic approach for different cancers by targeting multiple pathways involved in carcinogenesis.

Moreover, the prolonged release of Dox from MAH helps avoid the initial burst, which could lead to negative therapeutic effects. Dox-MAH effectively inhibited proliferation and induced apoptosis in SW480 cells, showing results comparable to Dox alone. The increase in the pro-apoptotic protein Bax and the decrease in the anti-apoptotic proteins Bcl-2 and procaspase-3 indicated that Dox-MAH promoted apoptosis through the disruption

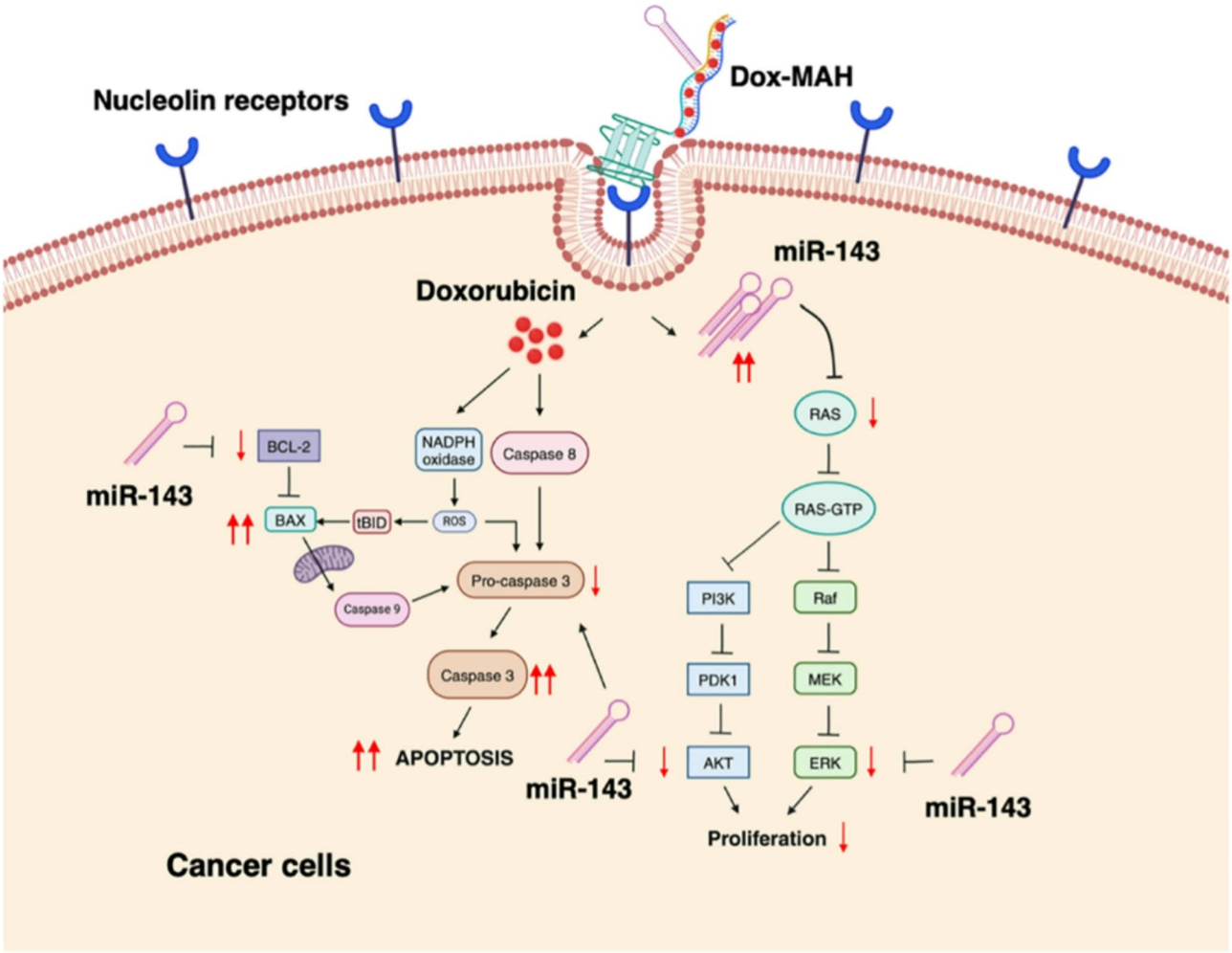

Fig. 8. Summary of the effects of Dox-MAH on the KRAS network and cell apoptosis signaling pathway.

of mitochondrial outer membrane permeability, leading to the activation of caspase-3. Previous studies have shown that Dox induces apoptosis in tumor cells, primarily through mitochondrial pathways. This process involves the release of cytochrome c from the mitochondria into the cytoplasm, where it forms an apoptosome, a multiprotein complex that includes cytochrome c, procaspase-9, and the adaptor protein Apaf-1. This complex activates caspase-3, causing cellular death substrates to be degraded[52]. The expression of procaspase-3 decreases as it is converted into active caspase-3 (Fig. 8).

However, a limitation of this research is that the reduction of adverse effects, such as cardiotoxicity, was not directly demonstrated. While AS1411 enhanced the specificity of MAH for CRC cells and Dox was shown to be non-toxic to normal colon cells, the direct impact of Dox-MAH on target tissues, including cardiac muscle and endothelial cells, remains unexamined. Therefore, further in vivo studies in animal models are required to evaluate the potential reduction of adverse effects and to confirm the efficacy of Dox-MAH in cancer treatment.

In summary, this study demonstrated that Dox-MAH effectively suppressed the growth of SW480 cells through apoptosis induction, with similar efficacy to Dox alone. The AS1411 aptamer enhances Dox toxicity, while having minimal impact on normal colon cells. Unlike single-target inhibitors, Dox-MAH provides a distinct advantage by targeting KRAS and its downstream signaling pathways, thereby reducing the likelihood of developing resistance.

Data availability

Any additional experimental data is available from the corresponding author upon reasonable request.

Received: 15 October 2024; Accepted: 12 March 2025
Published online: 27 March 2025

References

1. Sung, H. et al. Global cancer statistics 2020: GLOBOCAN estimates of incidence and mortality worldwide for 36 cancers in 185 countries. *Cancer J. Clin.* **71** (3), 209–249 (2021).
2. Chakrabarti, S. et al. Early stage colon cancer: current treatment standards, evolving paradigms, and future directions. *World J. Gastrointest. Oncol.* **12** (8), 808–832 (2020).
3. Dey, A. et al. Recent advancements, limitations, and future perspectives of the use of personalized medicine in treatment of colon cancer. *Technol. Cancer Res. Treat.* **22**, 15330338231178403 (2023).
4. Chabner, B. A. & Roberts, T. G. Jr Timeline: chemotherapy and the war on cancer. *Nat. Rev. Cancer*. **5** (1), 65–72 (2005).
5. Hanahan, D. & Weinberg, R. A. Hallmarks of cancer: the next generation. *Cell* **144** (5), 646–674 (2011).
6. Pérez-Herrero, E. & Fernández-Medarde, A. Advanced targeted therapies in cancer: drug nanocarriers, the future of chemotherapy. *Eur. J. Pharm. Biopharm.* **93**, 52–79 (2015).
7. Micura, R. & Höbartner, C. Fundamental studies of functional nucleic acids: aptamers, riboswitches, ribozymes and dnazymes. *Chem. Soc. Rev.* **49** (20), 7331–7353 (2020).
8. Chen, T. et al. Aptamer-conjugated nanomaterials for bioanalysis and biotechnology applications. *Nanoscale* **3** (2), 546–556 (2011).
9. Ireson, C. R. & Kelland, L. R. Discovery and development of anticancer aptamers. *Mol. Cancer Ther.* **5** (12), 2957–2962 (2006).
10. Breaker, R. R. DNA aptamers and DNA enzymes. *Curr. Opin. Chem. Biol.* **1** (1), 26–31 (1997).
11. Xu, Y. et al. Systematic evolution of ligands by exponential enrichment technologies and Aptamer-Based applications: recent progress and challenges in precision medicine of infectious diseases. *Front. Bioeng. Biotechnol.* **9**, 704077 (2021).
12. Wu, X. et al. Potential diagnostic and therapeutic applications of oligonucleotide aptamers in breast cancer. *Int. J. Mol. Sci.*. **18**(9). (2017).
13. Reyes-Reyes, E. M., Teng, Y. & Bates, P. J. A new paradigm for aptamer therapeutic AS1411 action: uptake by macropinocytosis and its stimulation by a nucleolin-dependent mechanism. *Cancer Res.* **70** (21), 8617–8629 (2010).
14. Cox, A. D. & Der, C. J. Ras history: the Saga continues. *Small GTPases*. **1** (1), 2–27 (2010).
15. Karnoub, A. E. & Weinberg, R. A. Ras oncogenes: split personalities. *Nat. Rev. Mol. Cell. Biol.* **9** (7), 517–531 (2008).
16. Shukla, S. et al. KRAS protein stability is regulated through SMURF2: UBCH5 complex-mediated β-TrCP1 degradation. *Neoplasia* **16** (2), 115–128 (2014).
17. Van Cutsem, E. et al. Fluorouracil, leucovorin, and Irinotecan plus cetuximab treatment and RAS mutations in colorectal cancer. *J. Clin. Oncol.* **33** (7), 692–700 (2015).
18. Liu, H. et al. Downregulation of miR–143 modulates KRAS expression in colorectal carcinoma cells. *Oncol. Rep.* **42** (6), 2759–2767 (2019).
19. Bartel, D. P. MicroRNAs: target recognition and regulatory functions. *Cell* **136** (2), 215–233 (2009).
20. Vasudevan, S., Tong, Y. & Steitz, J. A. Switching from repression to activation: MicroRNAs can up-regulate translation. *Science* **318** (5858), 1931–1934 (2007).
21. Guo, H. et al. The regulation of Toll-like receptor 2 by miR-143 suppresses the invasion and migration of a subset of human colorectal carcinoma cells. *Mol. Cancer*. **12**, 77 (2013).
22. Wang, L. et al. MiR-143 acts as a tumor suppressor by targeting N-RAS and enhances temozolomide-induced apoptosis in glioma. *Oncotarget* **5** (14), 5416–5427 (2014).
23. Zhang, H. et al. microRNA-143, down-regulated in osteosarcoma, promotes apoptosis and suppresses tumorigenicity by targeting Bcl-2. *Oncol. Rep.* **24** (5), 1363–1369 (2010).
24. Chen, X. et al. Role of miR-143 targeting KRAS in colorectal tumorigenesis. *Oncogene* **28** (10), 1385–1392 (2009).
25. Zhang, Y. et al. MicroRNA-143 targets MACC1 to inhibit cell invasion and migration in colorectal cancer. *Mol. Cancer*. **11**, 23 (2012).
26. Michael, M. Z. et al. Reduced accumulation of specific MicroRNAs in colorectal neoplasia. *Mol. Cancer Res.* **1** (12), 882–891 (2003).
27. Pigram, W. J., Fuller, W. & Hamilton, L. D. Stereochemistry of intercalation: interaction of daunomycin with DNA. *Nat. New. Biol.*. **235** (53), 17–19 (1972).
28. Saad Hmoud, A. & Awad Abdalla, M. Anticancer drugs' deoxyribonucleic acid (DNA) interactions. In *Biophysical Chemistry*, Ch. 6 (ed. Mohammed, A.A.K.) (IntechOpen, 2019).
29. Jawad, B. et al. Molecular mechanism and binding free energy of doxorubicin intercalation in DNA. *Phys. Chem. Chem. Phys.* **21** (7), 3877–3893 (2019).
30. Luksta, M. et al. Pressurized intraperitoneal aerosol chemotherapy (PIPAC) with cisplatin and doxorubicin in combination with FOLFOX chemotherapy as a first-line treatment for gastric cancer patients with peritoneal metastases: single-arm phase II study. *BMC Cancer*. **23** (1), 1032 (2023).
31. D'Ambrosio, L. et al. Doxorubicin plus Dacarbazine, doxorubicin plus Ifosfamide, or doxorubicin alone as a first-line treatment for advanced leiomyosarcoma: A propensity score matching analysis from the European organization for research and treatment of cancer soft tissue and bone sarcoma group. *Cancer* **126** (11), 2637–2647 (2020).
32. Zhao, N., Woodle, M. C. & Mixson, A. J. Advances in delivery systems for doxorubicin. *J. Nanomed. Nanotechnol.* **9**(5). (2018).
33. Thorn, C. F. et al. Doxorubicin pathways: pharmacodynamics and adverse effects. *Pharmacogenet. Genom.*. **21** (7), 440–446 (2011).
34. Semba, S., Mizuuchi, E. & Yokozaki, H. Requirement of phosphatase of regenerating liver-3 for the nucleolar localization of nucleolin during the progression of colorectal carcinoma. *Cancer Sci.* **101** (10), 2254–2261 (2010).
35. Lohlamoh, W., Soontornworajit, B. & Rotkrua, P. Anti-proliferative effect of doxorubicin-loaded AS1411 aptamer on colorectal cancer cell. *Asian Pac. J. Cancer Prev.* **22** (7), 2209–2219 (2021).
36. Balian, A. & Hernandez, F. J. Nucleases as molecular targets for cancer diagnosis. *Biomark. Res.* **9** (1), 86 (2021).
37. Huang, L. et al. KRAS mutation: from undruggable to druggable in cancer. *Signal. Transduct. Target. Ther.* **6** (1), 386 (2021).
38. Hopkins, A. L. Network pharmacology: the next paradigm in drug discovery. *Nat. Chem. Biol.* **4** (11), 682–690 (2008).
39. Singh, A. K. et al. Concept of hybrid drugs and recent advancements in anticancer hybrids. *Pharmaceuticals (Basel)*. **15**(9) (2022).
40. Rotkrua, P. et al. A molecular hybrid comprising AS1411 and PDGF-BB aptamer, cholesterol, and doxorubicin for inhibiting proliferation of SW480 cells. *J. Mol. Recognit.* **34** (11), e2926 (2021).
41. Toden, S., Zumwalt, T. J. & Goel, A. Non-coding RNAs and potential therapeutic targeting in cancer. *Biochim. Biophys. Acta Rev. Cancer*. **1875** (1), 188491 (2021).
42. Reyes-Reyes, E. M. et al. Mechanistic studies of anticancer aptamer AS1411 reveal a novel role for nucleolin in regulating Rac1 activation. *Mol. Oncol.* **9** (7), 1392–1405 (2015).
43. Soundararajan, S. et al. The nucleolin targeting aptamer AS1411 destabilizes Bcl-2 messenger RNA in human breast cancer cells. *Cancer Res.* **68** (7), 2358–2365 (2008).
44. Akao, Y. et al. Impairment of K-Ras signaling networks and increased efficacy of epidermal growth factor receptor inhibitors by a novel synthetic miR-143. *Cancer Sci.* **109** (5), 1455–1467 (2018).
45. McCubrey, J. A. et al. Roles of the RAF/MEK/ERK and PI3K/PTEN/AKT pathways in malignant transformation and drug resistance. *Adv. Enzyme Regul.* **46**, 249–279 (2006).
46. Wu, J. et al. Biological functions and potential mechanisms of miR–143–3p in cancers (Review). *Oncol. Rep.*. **52**(3). (2024).
47. Sugito, N., Heishima, K. & Akao, Y. Chemically modified MIR143-3p exhibited anti-cancer effects by impairing the KRAS network in colorectal cancer cells. *Mol. Ther. Nucleic Acids*. **30**, 49–61 (2022).

48. Borralho, P. M. et al. MicroRNA-143 reduces viability and increases sensitivity to 5-fluorouracil in HCT116 human colorectal cancer cells. *Febs J.* **276** (22), 6689–6700 (2009).
49. Karimi, L. et al. Function of microRNA-143 in different signal pathways in cancer: new insights into cancer therapy. *Biomed. Pharmacother.* **91**, 121–131 (2017).
50. Tavanafar, F. et al. Restoration of miR-143 expression could inhibit migration and growth of MDA-MB-468 cells through down-regulating the expression of invasion-related factors. *Biomed. Pharmacother.* **91**, 920–924 (2017).
51. Green, A. R. et al. MYC functions are specific in biological subtypes of breast cancer and confers resistance to endocrine therapy in luminal tumours. *Br. J. Cancer.* **114** (8), 917–928 (2016).
52. Riedl, S. J. & Salvesen, G. S. The apoptosome: signalling platform of cell death. *Nat. Rev. Mol. Cell. Biol.* **8** (5), 405–413 (2007).

Acknowledgements

This research was supported by Thailand Science Research and Innovation (TSRI) Fundamental Fund, fiscal year 2024 [Contract No. TUFF 49/2567], Faculty of Medicine, Thammasat University [Contract No. 2-11/2566], National Research Council of Thailand (NRCT) [Contract No. N41A671022], and Thammasat University Research Unit in Innovation of Molecular Hybrid for Biomedical Application. The authors gratefully thank Mr. Michael Jan Everts, Clinical Research Center, Faculty of Medicine, Thammasat University, for comments on the manuscript.

Author contributions

K.L.: Data curation, methodology, funding acquisition, writing—original draft preparation; B.S.: Conceptualization, formal analysis, writing—reviewing and editing; J.A.: Methodology, writing—reviewing and editing; P.R.: Conceptualization, formal analysis, funding acquisition, investigation, supervision, writing—reviewing and editing. All authors reviewed the manuscript and approved the final version.

Declarations

Competing interests

The authors declare no competing interests.

Additional information

Supplementary Information The online version contains supplementary material available at https://doi.org/10.1038/s41598-025-94159-y.

Correspondence and requests for materials should be addressed to P.R.

Reprints and permissions information is available at www.nature.com/reprints.

Publisher's note Springer Nature remains neutral with regard to jurisdictional claims in published maps and institutional affiliations.